Vision, Modeling, and Visualization (2011)
Peter Eisert, Konrad Polthier, and Joachim Hornegger (Eds.)

The Recognition of Ethnic Groups based on Histological Skin Properties

C. Malskies[1] and E. Eibenberger[1,2,3] and E. Angelopoulou [1,2]

[1] Pattern Recognition Lab, University of Erlangen-Nuremberg, Germany
[2] Erlangen Graduate School in Advanced Optical Technologoies (SAOT), Erlangen, Germany
[3] International Max Planck Research School for Optics and Imaging

Abstract

We present an algorithm to recognize ethnic groups based on biologically justified features, such as melanin or hemoglobin concentrations. These biophysical features are extracted from skin reflectance spectra and allow, in contrast to technical features, a medical interpretation and intuitive rating of the recognition results. For this purpose, a physics-based light transport model for skin is required. We use an existing model based on Kubelka-Munk theory, which is physically accurate and computationally tractable. The evaluation of the ethnicity classification reveals that in comparison to an approach, directly based on the reflectance spectra, our proposed biophysical classification is slightly better. To reduce computation time we analyze the impact of spectral band reduction on the ethnicity classification and show that this can be achieved on the expense of only a small accuracy loss.

Categories and Subject Descriptors (according to ACM CCS): I.4.1 [Image Processing and Computer Vision]: Digitzation and Image Capture—Reflectance I.4.8 [Image Processing and Computer Vision]: Scene Analysis—Color

1. Introduction

Due to increasing security concerns, the application field of biometric recognition is spreading more and more in the last years. A popular and highly researched biometric security application are face recognition systems, as they offer a non-intrusive and natural way of identification [KHA*05]. To further increase the distinctness between individuals, algorithms based on hyperspectral images are investigated (e.g. [PHPT03, CYK*09, AHC10]).

Compared to common images, consisting of one or three channels (grayscale or RGB), hyperspectral images can be considered as an image "cube" containing a multitude of bands. Each channel of the cube corresponds to the sensor response at a certain wavelength. Therefore, hyperspectral images simultaneously provide spatial and spectral information and, thus, provide a very comprehensive representation of the scene reflectance. The spectral response at an individual pixel is highly caused by the underlying material. As the chemical composition of a material often results in an individual spectral signature, hyperspectral images are widely used for material identification (e.g. in art [PMRP08] or remote sensing [RX06]).

The highly discriminative information of hyperspectral data is used in face recognition to obtain an increased performance, e.g. [PHPT03, CYK*09, AHC10]. To support the biometric recognition process, algorithms are developed to classify faces or skin into ethnic groups. Their essential idea is that the color appearance of skin is mainly caused by the two chromophores, melanin and hemoglobin [BK10]. The differences between ethnicities are predominantly effected by varying melanin concentrations: Darker skin, like African skin, is provoked by an increased light absorption due to a higher melanin fraction. In Caucasian skin, in contrast, the lower melanin concentration results in a brighter skin appearance [Raw06].

There are two categories of ethnicity recognition approaches based on skin reflectance. Firstly, the reflectance spectra of skin can be used directly as feature vectors for classification. Pan et al. [PHPT03] apply this idea to normalized skin spectra in the near-infrared range and distinguish skin of three ethnic groups ("Asian", "African", "Caucasian"). Secondly, not the spectra themselves are employed, but a set of features is extracted from the skin reflectance curves. Huynh and Robles-Kelly [HRK10] com-

DOI: 10.2312/PE/VMV/VMV11/353-360

pute NURBS-based descriptors and features based on Gaussian mixture modelling [AMD01] to recognize "Caucasian", "Indian" and "Oriental" ethnicities.

Our proposed approach for recognizing ethnic groups belongs the second category based on feature extraction. However, in contrast to the existing methods, which are based on technical features (e.g. the parameters of NURBS), we extract histological skin properties, like chromophore concentrations or skin layer thicknesses, and employ those medical characteristics during the classification process. Therefore, we directly exploit the biological reasons for skin appearance variations between different ethnicities. Furthermore, biologically justified decisions allow a more intuitive interpretation of the results.

The extraction of medical skin properties requires a skin reflectance model based on the interaction of light with the tissue. As skin has a layered structure of several translucent slabs containing various chromophores and other structures, like cell membranes and organelles, the model has to capture absorption and scattering processes. In computer vision and computer graphics a huge variety of skin reflectance models are proposed, ranging from simplistic to physically precise. Tsumura et al. [THM99] disregard the layered structure of the skin and simply model its reflectance as a linear combination of the both pigments hemoglobin and melanin. In contrast, Claridge and Cotton [CC96] take account of the individual layers with their prominent absorbers and scatterers and provide a BRDF model based on the physics-based Kubelka-Munk theory [KM31]. Donner and Jensen [DJ06] base the light transport inside the tissue on diffusion processes and provide a physically-precise BSSRDF. Finally, approaches based on Monte Carlo techniques (e.g. [KB04]) simulate the path of single photons and, thus, are physically precise, yet, computationally expensive.

As a compromise between physical accuracy and computational tractability, our extraction of histological tissue properties is based on the Kubelka-Munk model by Claridge and Cotton [CC96]. Based on this model we analyze the performance of our proposed ethnicity recognition using biophysical skin properties as features. An important aspect of the evaluation is the suitability of existing skin reflectance models for covering the biological variations between skin of different ethnicities.

In the next section we start with an overview of the medical background on skin histology.Sec. 3 provides the theory of the Kubelka-Munk theory for skin reflectance modelling. Sec. 4 describes the classification of ethnic groups based on biophysical characteristics. The evaluation is presented in Sec. 5, before Sec. 6 concludes this paper.

2. Optical Properties of Skin

Besides reflection and refraction, the two most important interactions of light with matter are absorption and scattering.

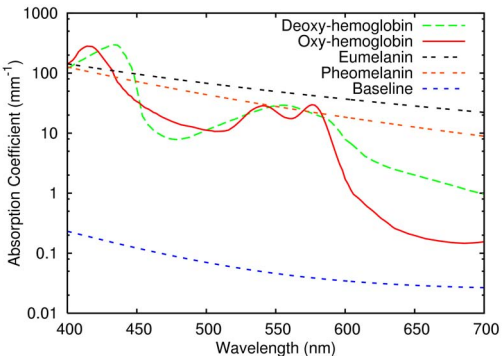

Figure 1: *Absorption spectra of different absorbers.*

The light transport through a purely absorbing material can be described with Beer-Lambert's law, stating that the incoming radiant intensity I_i is attenuated according to

$$I_o = e^{-\sigma_a d} I_i. \quad (1)$$

Here, I_o is the outgoing intensity and d is the pathlength. σ_a is the wavelength-dependent *absorption coefficient* of the material per unit pathlength. Light may also be deflected while passing through a material. This is referred to as scattering and is caused by collisions with molecules or particles. The ability of a material to scatter light is described by the *scattering coefficient* σ_s. In skin optics, there are two types of scattering: *Rayleigh scattering* and *Mie scattering*. While Rayleigh scattering is caused by molecules or particles much smaller than the light's wavelength, Mie scattering is caused by particles of approximately the same size. For human skin, the scattering coefficient of Rayleigh scattering $\sigma_s^{Rayleigh}(\lambda)$ at a wavelength λ is given by

$$\sigma_s^{Rayleigh}(\lambda) = 2.0 \times 10^{11} \times \lambda^{-4} [mm^{-1}]. \quad (2)$$

The formula for the Mie scattering coefficient $\sigma_s^{Mie}(\lambda)$ is

$$\sigma_s^{Mie}(\lambda) = 2.0 \times 10^{4} \times \lambda^{-1.5} [mm^{-1}]. \quad (3)$$

In skin optics studies, skin is commonly modeled as consisting of two main layers: the *epidermis* and the *dermis* [BK10]. Beside prominent absorbing chromophores, which are described in the following subsections, skin has some baseline absorption due to structures like organelles and cell membranes. The baseline absorption $\sigma_a^{base}(\lambda)$ can be computed with [DJ06]

$$\sigma_a^{baseline}(\lambda) = 0.0244 + 8.53 e^{-(\lambda - 154)/66.2} \ [mm^{-1}]. \quad (4)$$

2.1. Epidermis

The epidermis is the outermost layer of the human skin. Its thickness ranges from about 0.027 mm up to 0.15 mm and varies extremely between different individuals and even between body regions [BK10]. Melanin is the most prominent

absorber within the epidermis and exists as three different types: the light brown and dark brown/black *eumelanin* and the yellow/red *pheomelanin*. The absorption coefficient σ_a^{em} of both eumelanin types can be computed with [DJ06]

$$\sigma_a^{em}(\lambda) = 6.6 \times 10^{10} \times \lambda^{-3.33} \quad [mm^{-1}]. \tag{5}$$

The absorption coefficient of pheomelanin σ_a^{pm} is given by

$$\sigma_a^{pm}(\lambda) = 2.9 \times 10^{14} \times \lambda^{-4.75} \quad [mm^{-1}]. \tag{6}$$

Most individuals produce a combination of both types. Therefore, a melanin type blend β_m is introduced to describe the ratio of eumelanin to pheomelanin. The total epidermal absorption coefficient $\sigma_a^{epi}(\lambda)$ can then be modeled with

$$\sigma_a^{epi}(\lambda) = C_m \left[\beta_m \sigma_a^{em}(\lambda) + (1-\beta_m)\sigma_a^{pm}(\lambda)\right] + (1-C_m)\sigma_a^{baseline}(\lambda) \quad [mm^{-1}]. \tag{7}$$

C_m is the melanin fraction and β_m the melanin type blend.

2.2. Dermis

Beneath the epidermis is the dermis, which is a 0.6 to 3 mm thick layer that can be divided in two sublayer, the *papillary dermis* and the *reticular dermis* [BK10]. The prominent chromophore of the dermis, the hemoglobin, is located inside the red blood corpuscles. Hemoglobin exists in two states: oxygenated and deoxygenated. Both types have absorption peaks at a wavelength of about 550 nm, where the oxygenated hemoglobin forms a characteristic w-shape (see Fig. 1). In the arteries, 90 - 95% of the hemoglobin is oxygenated, while only 47% is oxygenated in veins. Thus, the overall ratio γ of oxygenated to deoxygenated hemoglobin is 0.6 - 0.8. The total volume fraction of hemoglobin C_h in the whole dermis is given with 0.2 - 7% [BK10]. The dermal absorption coefficient $\sigma_a^{derm}(\lambda)$ can be computed with [DJ06]

$$\sigma_a^{derm}(\lambda) = C_h \left[\gamma \sigma_a^{oxy}(\lambda) + (1-\gamma)\sigma_a^{deoxy}(\lambda)\right] + (1-C_h)\sigma_a^{baseline}(\lambda) \quad [mm^{-1}], \tag{8}$$

where σ_a^{oxy} is the absorption coefficient of oxygenated and σ_a^{deoxy} of deoxygenated hemoglobin.

2.3. Ethnic Differences in Skin Pigmentation

Skin reflectance measurements revealed that European skin is the lightest skin type, closely followed by Chinese and Mexican skin. Indian skin is significantly darker, while African skin is the darkest [AAB*02].

The source of these skin color variations are two biological chromophores: hemoglobin and melanin [BK10]. In general, the most darkly pigmented skin types, i.e. Indian and African, have about twice as much epidermal melanin as lightly pigmented skin types, e.g. European and Chinese [AAB*02]. However, three different subtypes of melanin have to be distinguished: light colored yellow/red pheomelanin, light brown eumelanin (alkali soluble) and dark brown/black eumelanin (alkali insoluble) [Raw06]. Although lightly pigmented skin has approximately half as much melanin as darkly pigmented skin, its melanin composition contains about three times more lightly colored alkali soluble eumelanin [Raw06]. In contrast, the darkest skin types have significantly more dark black/brown alkali insoluble eumelanin [AAB*02]. Due to the smaller melanin concentration in the epidermis of Caucasian skin, the absorption characteristics of hemoglobin inside the dermis contribute to the pinkish color of Caucasians. Furthermore, carotenes are the source of yellow/orange pigmentation [Raw06].

Besides the quantitative differences of the melanin types, ethnic variations exist regarding the packaging of melanin (melanosomes) inside the epidermis. In darker skin the melanin tends to be packaged into larger melanosomes, whereas in lighter skin the melanosome size tends to be smaller. So far, it is unclear how these structural differences influence the skin color [AAB*02], respectively the scattering processes.

3. Skin Reflectance Modeling

The extraction of biologically justified features requires a physics-based model, which is able to describe the light transport within skin. Nevertheless, a tradeoff between physical accuracy and computational tractability must be found. We decided for the skin reflectance model by Claridge and Cotton [CC96], which is based on Kubelka-Munk theory. In this section we will present this physics-based model.

3.1. Kubelka-Munk Theory

The Kubelka-Munk theory [KM31] describes the absorption and scattering of light within pigmented materials. It relates the absorption and scattering coefficients of individual thin layers to an overall reflectance [BK10]. The basis are two oppositely directed fluxes within the material. One flux I is directed into increasing depth and the other flux J is directed back to the surface, due to scattering of light within the material. As forward scattering is indistinguishable from no scattering, fluxes cannot change their directions. Hence, light is either transmitted further into the material or scattered back to the surface. The change in flux at a certain distance x from the surface over an infinitesimal distance dx is

$$dI = -\sigma_a a_0 I dx - \sigma_s a_0 I dx + \sigma_a b_0 J dx, \tag{9}$$

$$dJ = \sigma_a a_0 J dx + \sigma_s a_0 J dx - \sigma_a b_0 I dx, \tag{10}$$

where the constants a_0 and b_0 relate dx to the average path lengths for I and J [CC96]. Assuming directionally isotropic radiation due to high scattering and that J is zero at a distance $x = d$ (d is the slab thickness), Eq. 9 and Eq. 10 can be solved by exponential functions [EH79], leading to

$$R(\beta, K, d) = \frac{(1-\beta^2)(e^{Kd} - e - Kd)}{(1+\beta)^2 e^{Kd} - (1-\beta)^2 e^{-Kd}}, \tag{11}$$

$$T(\beta,K,d) = \frac{4\beta}{(1+\beta)^2 e^{Kd} - (1-\beta)^2 e^{-Kd}}, \quad (12)$$

where $K = \sqrt{4\sigma_a^2 + 8\sigma_a\sigma_s}$ and $\beta = \sqrt{\frac{2\sigma_a}{2\sigma_a+4\sigma_s}}$. The transmittance T corresponds to I at the bottom ($x = d$) and the reflectance R to J at the surface ($x = 0$) of the slab. Eq. 11 and Eq. 12 can be considered as an extension to Beer-Lambert's law: for a non-scattering material $\sigma_s = 0$ and, hence, they resolve to $R(\beta,K,d) = 0$ and $T(\beta,K,d) = e^{-2\sigma_a d}$ (cp. Eq. 1).

3.2. Model of the Epidermis

As only about 5% of incident radiation is directly reflected at the epidermis and the amount of backscattered light is negligible [AP81], Claridge and Cotton [CC96] assume the epidermis to be non-scattering. Then, light is only transmitted through the epidermis, where it gets attenuated due to absorption. This can be modeled with Beer-Lambert's law: The ratio $\Theta(\sigma_a^{epi}, d)$ of incident to transmitted radiation is

$$\Theta(\sigma_a, d) = e^{-\sigma_a^{epi} d}. \quad (13)$$

3.3. Model of the Dermis

As the epidermis is assumed to be non-scattering, all light that is not absorbed must be transmitted to the dermis. To account for structural differences inside the dermis, Claridge and Cotton divide the dermis in threes sublayers: the upper and lower papillary dermis and the reticular dermis. The lowermost layer, the reticular dermis, contains larger structures. Therefore, strong forward directed Mie scattering occurs, which is indistinguishable from no scattering (cp. Sec. 3.1). Hence, light reaching the reticular dermis will never return to the surface. Both papillary layers are modeled with the Kubelka-Munk theory to cover scattering and absorption processes. The prevailing scattering type is Rayleigh scattering. Due to different blood vessel sizes, the upper papillary dermis contains a higher hemoglobin concentration than the lower papillary dermis. Claridge and Cotton model this hemoglobin concentration ration as well as the ratio of the thickness of the upper to lower papillary dermis as a constant δ (the papilary dermis ratio). See [CC96] for more details on these assumptions.

Light that is not reflected at the upper papillary dermis is transmitted to the lower papillary dermis. There, it is either reflected back to the upper papillary dermis or transmitted as well. The reflected part of light is then again reflected or transmitted at the upper layer and so on. Therefore, the total reflectance of the papillary dermis R_{pd} is

$$R_{pd} = R_{ud} + T_{ud}R_{ld}T_{ud} + T_{ud}R_{ld}R_{ud}R_{ld}T_{ud} + \dots. \quad (14)$$

R_{ud} and T_{ud} are the reflectance and transmittance of the upper papillary dermis and R_{ld} is the transmittance of the lower papillary dermis. The reflectance and transmittance can be computed using Eq. 11 and Eq. 12. The absorption and scattering coefficients are given by Eq. 8 and Eq. 2. Note that

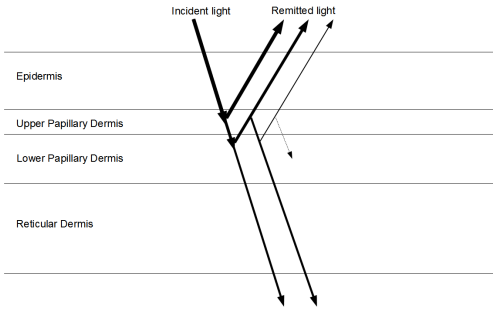

Figure 2: *Light transport through human skin.*

this is a geometric series. Assuming $R_{ud} < 1$ and $R_{ld} < 1$, this series converges to

$$R_{pd} = R_{ud} + \frac{T_{ud}R_{ld}T_{ud}}{1 - R_{ud}R_{ld}}. \quad (15)$$

3.4. Layered Skin

Light reaching the papillary dermis has to pass the absorbing epidermis. Afterwards, remitted light from the papillary dermis has to pass the epidermis again in order to leave the skin. To take into account the epidermal absorptivity, the total remitted light from the entire skin has to be scaled. The finally emitted light R_{total} can be computed with [CC96]

$$R_{total} = R_{pd}\Theta^2 \quad (16)$$

using the appropriate absorption and scattering coefficients. As all coefficients are wavelength dependent, Eq. 16 has to be evaluated for each considered wavelength. The schematic structure of the entire skin model is shown in Fig. 2.

4. Classification of Ethnicities

The goal of this work is the classification of ethnicities based on biologically justified features. These features have the advantage that they can be interpreted in a medical manner and also provide an intuitive interpretation of the classification result. Furthermore, the biophysical features directly exploit the biological reasons for skin appearance variations between different ethnicities. To model the interaction of light with the skin tissue, we chose the skin reflectance model by Claridge and Cotton [CC96], as it is physical precise but still of tractable complexity.

The extraction of the histological features is obtained by evaluating different parameter combinations. Given a set of parameters, Eq. 7 and 8 are used to compute the epidermal and dermal absorption coefficients. Both coefficients, in conjunction with the scattering coefficient (Eq. 2), are then combined to compute a reflectance spectrum by evaluating

	Range	Stepsize	Description
C_m	0.0 - 0.5	0.01	Melanin fraction
β_m	0 - 1	0.1	Melanin type blend
C_h	0.001 - 0.1	0.001	Hemoglobin fraction
γ	0.75		Oxygenation ratio
δ	0.75		Papillary dermis ratio
d_{epi}	0.05 - 0.15	0.05	Epidermal thickness
d_{derm}	0.5 - 3.0	0.1	Dermal thickness

Table 1: *Biological parameters with default values.*

Eq. 16. As all coefficients are wavelength-dependent, the total reflectance has to be evaluated for each considered λ.

Given a certain skin spectrum as input, the parameter combination is searched which minimizes the sum-of-squared-distances (SSD) between the input spectrum and the computed output spectrum. The SSD is given by

$$SSD = \sum_{\lambda=400}^{700} (R_\lambda^{in} - R_\lambda^{out})^2, \qquad (17)$$

where R_λ^{in} is the reflectance intensity of the given spectrum at the wavelength λ and R_λ^{out} is the reflectance intensity of the computed spectrum at λ. To find the biological parameters which minimize the SSD, a set of possible parameter combinations is evaluated. The parameter set resulting in the smallest SSD error is considered as the output of the extraction process. Tab. 1 summarized the tested ranges and step sizes of the default parameters, which were evaluated for the extraction of the biological values. The oxygenation ratio γ is constant at $\gamma = 0.75$, as it varies only marginally between individuals [DJ06].

In our classification of ethnic groups we discriminate between Caucasian, Asian and African skin. Fig. 3 shows examples of skin reflectances for each skin type. As mentioned in Sec. 2.3, Caucasian skin has the lightest appearance and, hence, the highest reflectivity. Due to their higher melanin concentrations, Asian and African skin reflectances are lower. The melanin fraction C_m typically ranges from 1.3% for very pale tanned individuals up to 43% for very dark pigmented individuals, e.g. Africans. The melanin type blend β_m ranges from 0.049 to 0.36 and varies from individual to individual with high intersections between ethnicities or rather skin types like well or pale tanned [BK10].

An analysis of the extracted features showed that the estimated melanin type blend β_m and epidermal thickness d_{epi} are unsuitable features for classification of ethnicities, as they stay almost constant for all spectra (see Sec. 5.1 for more details). Therefore, we focused on the remaining three features, namely the melanin fraction C_m, the hemoglobin fraction C_h and the dermal thickness d_{derm}. Fig. 4 shows scatter plots of these biophysical parameters for the three ethnic groups. Especially, the African skin is clearly separated from the others. Furthermore, the clusters of Caucasian and Asian skin are overlapping.

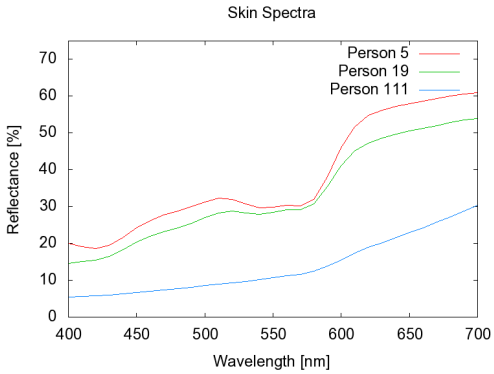

Figure 3: *Reflectance spectra of the three ethnic groups: Caucasian (red), Asian (green), African (blue).*

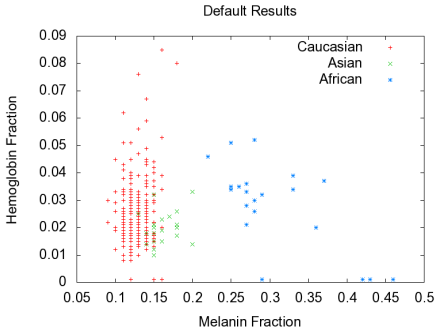

(a) Melanin fraction C_m and hemoglobin fraction C_h

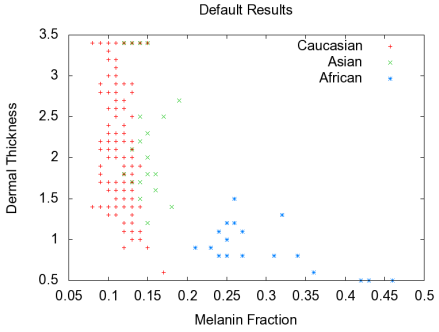

(b) Melanin fraction C_m and dermal thickness d_{derm}.

Figure 4: *Scatter plot of different histological properties for Caucasian (red), Asian (green) and African skin (blue).*

For classification we used a multilayer perceptron classifier [DHS00]. A single perceptron defines a linear boundary in feature space and can be used to detect on which side a

feature vector is. A multilayer perceptron typically has an input layer, which defines the linear boundaries. A second (hidden) layer can then be trained such that it combines these boundaries with logical "AND" operations to define different areas in feature space. Furthermore, a third (output) layer combines these enclosed areas with logical "OR" operations to define clusters belonging to a certain class.

5. Evaluation

For the evaluation of the classification of ethnic groups, the University of Oulu Physics-Based Face Database [MMSP00] was used. It contains 345 skin reflectance spectra of 111 individuals, with 300 spectra of Caucasian, 24 spectra of Asian and 21 spectra of African skin. The reflectance curves are provided in the wavelength range from 400 to 700 nm with a step size of 10 nm.

To analyze the suitability of the skin reflectance model for a reliable estimation of histological parameters, firstly, an evaluation of the extracted biophysical values is provided. Afterwards, the classification of ethnic groups is evaluated. Here, we provide a comparison to the approach similar to that of Pan et al. [PHPT03], where the skin spectra are used directly as feature vectors. Finally, an evaluation of the impact of band selection on the performance of parameter extraction and ethnicity classification is provided.

5.1. Evaluation of the Estimation of Tissue Histology

Based on the previous assumptions about tissue histological properties of ethnic groups, the first step is to verify whether the estimated values lie within a reasonable range from a biological point of view.

Firstly, we observed that the estimated melanin type blend β_m remains constant at $\beta_m = 1$ for all input spectra, meaning that epidermal melanin is entirely composed of eumelanin. This, however, contradicts medical conditions [Raw06]. This misestimation is caused by the featureless and very similar absorption spectra of eumelanin and pheomelanin, which make a discrimination between both types difficult. Furthermore, the epidermal thickness is constantly estimated as $d_{epi} = 0.05$ mm, except of a few outliers. Due to the non-scattering assumption of the epidermis in the Kubelka-Munk model, light transport within the epidermis is modeled with Beer-Lambert's law. This directly relates the absorption coefficient to the path length. Hence, to achieve a certain intensity one can either decrease the absorption coefficient and increase the pathlength or vice versa. Due to implementation details, a short pathlength (i.e. thickness) was tested first, which explains the epidermal thickness values.

For the remaining parameters, the mean values and standard deviations of all spectra of an ethnic group are presented in Tab. 2. Their minimum and maximum values are listed as well. Due to the lack of medical ground truth, it is not possible to quantify the accuracy of the histological parameters. However, the results are reasonable in a general medical sense [BK10]. As expected, African skin is predicted with the highest and Caucasian skin with lowest melanin concentration C_m. Furthermore, the melanin concentration in Asian skin is closer to Caucasian than to African skin, fulfilling histological expectations [AAB*02]. As already mentioned, the melanin fraction can be controlled by fixing the epidermal thickness at some value. This would require some medical reference data to calibrate the Kubelka-Munk model.

Caucasian	C_m	C_h	d_{derm}	SSD
Mean	0.109	0.0285	2.4743	0.047
Std. Dev.	0.0109	0.0086	0.4915	
Min	0.05	0.011	0.6	0.0232
Max	0.17	0.076	2.9	0.093
Asian				
Mean	0.1438	0.0187	2.05	0.0346
Std. Dev.	0.0152	0.0046	0.425	
Min	0.12	0.011	1.2	0.0212
Max	0.19	0.031	2.9	0.0473
African				
Mean	0.2919	0.0243	0.9333	0.0266
Std. Dev.	0.0568	0.0076	0.2254	
Min	0.21	0.001	0.5	0.0201
Max	0.46	0.036	1.5	0.0308

Table 2: *Results using default parameters.*

Comparing the SSD errors between the estimated and the input skin spectra, it is observable that Caucasian skin is predicted with the highest SSD error, followed by Asian skin and, finally, African skin with the smallest error. This is caused by higher magnitudes of Caucasian and Asian skin reflectance, compared to African skin. However, this does not lead to a higher accuracy for the results of African skin.

The impact of the non-scattering assumption of the epidermis is illustrated in Fig. 5. The difference between a given spectrum and the estimated spectrum is high at small wavelengths, where the absorption is the strongest (see Fig. 1). Modeling the epidermis as scattering, would result in a direct reflection of some of the light back to the surface and would balance this effect.

5.2. Evaluation of the Classification of Ethnic Groups

For ethnicity classification based on three biological quantities (melanin fraction C_m, hemoglobin fraction C_h and dermal thickness d_{derm}), the Java-based WEKA framework of the University of Waikato [HBF*09] was used. As classifier a multilayer perceptron was used and evaluated with a 10-fold cross validation test.

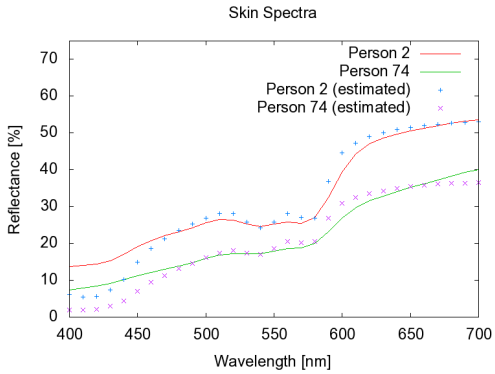

Figure 5: *Example spectra of Caucasian (person 2) and African (person 74) skin and the estimated spectra.*

Caucasian	Asian	African	classified as
296	4	0	Caucasian
8	16	0	Asian
0	0	21	African

Table 3: *Confusion matrix of the classification using default parameters. Classification rate: 96.52%.*

With the default setup, 333 spectra are classified correctly, which is equivalent to a recognition rate of 96.52%. The classification result is summarized in the confusion matrix of Tab. 3. As expected, African skin is classified entirely correct, because the melanin fractions and the dermal thicknesses of African skin are clearly separated from Caucasian and Asian skin. However, Caucasian and Asian skin are not separated equally precise, as the features of both skin types have more overlapping clusters. This might be caused by the loss of melanin type blend information (β_m) and the fact that not both eumelanin types are covered by the skin model.

If the reflectance spectra are directly used for classification [PHPT03], the classification rate is marginally lower with 96.23%. The confusion matrix of this approach is shown in Tab. 4. Although, this method still produces comparable classification results, it lacks the possibility of an intuitive histological interpretation of the decision. Therefore, the approach based on biologically-justified features is preferred as we can argue medically for an obtained result.

5.3. Evaluation of the Impact of Band Selection

In order to reduce memory and time consumptions, one can reduce the number of frequency bands of the reflectance spectra. Therefore, we analyzed the impact of choosing different combinations of wavelength bands. The seven frequency bands, which produced the best results, are presented in Tab. 6. Tab. 5 shows the results of the parameter estimation when only these seven frequency bands are used for the extraction. Although the SSD values are almost twice as high as the default values, the classification rate is marginally smaller with 96.23%. As Tab. 7 shows the respective confusion matrix and reveals that the result is comparable to the full frequency resolution results. Wang and Angelopoulou [WA06] presented a method to select the most informative frequency bands from a spectrum. According to their work, for skin the seven frequency bands with the highest information content are at 430, 530, 580, 590, 600, 650 and 690 nm. The confusion matrix is shown in Tab. 8. The classification rate of 95.07% is slightly smaller with these frequency bands. The reason is that these bands were chosen subject to an optimal distinction between skin and non-skin materials, whereas we want to distinct several skin groups. Hence, it is preferable to use equidistant frequency bands, which are evenly distributed over the visible spectrum.

Caucasian	Asian	African	classified as
292	7	1	Caucasian
5	19	0	Asian
0	0	21	African

Table 4: *Confusion matrix of the classification using spectral reflections directly. Classification rate: 96.23%.*

Caucasian	C_m	C_h	d_{derm}	SSD
Mean	0.084	0.092	1.034	0.1014
Std. Dev.	0.032	0.013	0.182	
Min	0.02	0.047	0.5	0.068
Max	0.28	0.099	1.6	0.15
Asian				
Mean	0.163	0.06	0.875	0.0776
Std. Dev.	0.041	0.013	0.094	
Min	0.09	0.039	0.7	0.0539
Max	0.25	0.099	1.1	0.1071
African				
Mean	0.409	0.025	0.633	0.0479
Std. Dev.	0.057	0.018	0.128	
Min	0.32	0.001	0.5	0.0343
Max	0.49	0.052	0.9	0.058

Table 5: *Results using the frequency bands of Tab. 6.*

6. Conclusions

Our proposed approach for ethnicity classificaton is based on biologically justified skin features, like hemoglobin or

Band #	1	2	3	4	5	6	7
λ [nm]	400	450	500	550	600	650	700

Table 6: *Selection of seven frequency bands.*

Caucasian	Asian	African	classified as
294	5	1	Caucasian
7	17	0	Asian
0	0	21	African

Table 7: *Confusion matrix of the classification using the 7 bands of Tab. 6. Classification rate: 96.23%.*

Caucasian	Asian	African	classified as
295	5	1	Caucasian
9	14	1	Asian
0	2	19	African

Table 8: *Confusion matrix of the classification using the 7 bands of [WA06]. Classification rate: 95.07%.*

melanin concentrations, which are extracted from skin reflectance spectra. Compared to the direct use of the spectra, our histological properties resulted in a slightly better classification performance and are preferable, as one can argue biologically for an obtained result. While African and Caucasian skin is mostly classified correctly, there are missclassfications of Asians. To address this problem, we assume that a further refinement of skin reflectance models to better capture the different types of melanin could help. Furthermore, the incorporation of carotene could provide further discriminative information. Our analysis of spectral band selection, in order to reduce computational complexity, resulted in an only marginally lower classification performance.

7. Acknowledgments

The authors gratefully acknowledge funding of the Erlangen Graduate School in Advanced Optical Technologies (SAOT) by the German National Science Foundation (DFG) in the framework of the excellence initiative. E. Eibenberger is supported by the International Max Planck Research School for Optics and Imaging.

References

[AAB*02] ALALUF S., ATKINS D., BARRETT K., BLOUNT M., CARTER N., HEATH A.: Ethnic Variation in Melanin Content and Composition in Photoexposed and Photoprotected Human Skin. *Pigment Cell Research 15*, 2 (2002), 112–118. 3, 6

[AHC10] ARANDJELOVIC O., HAMMOUD R. I., CIPOLLA R.: Thermal and Reflectance Based Personal Identification Methodology under Variable Illumination. *Pattern Recognition 43*, 5 (2010), 1801–1813. 1

[AMD01] ANGELOPOULOU E., MOLANA R., DANIILIDIS K.: Multispectral Skin Color Modeling. In *IEEE Computer Society Conference on Computer Vision and Pattern Recognition* (2001), pp. 635–642. 2

[AP81] ANDERSON R. R., PARRISH J. A.: The Optics of Human Skin. *The Journal of Investigative Dermatology 77*, 1 (1981), 13–19. 4

[BK10] BARANOSKI G. V. G., KRISHNASWAMY A.: *Light & Skin Interactions: Simulation for Computer Graphics Applications*. Morgan Kaufmann, 2010. 1, 2, 3, 5, 6

[CC96] CLARIDGE E., COTTON S. D.: Developing a Predictive Model of Human Skin Colouring. In *SPIE Proceedings Vol. 2708 Medical Imaging 1996: Physics of Medical Imaging* (1996), pp. 814–825. 2, 3, 4

[CYK*09] CHANG H., YAO Y., KOSCHAN A., ABIDI B. R., ABIDI M. A.: Improving Face Recognition via Narrowband Spectral Range Selection using Jeffrey Divergence. *IEEE Transactions on Information Forensics and Security 4*, 1 (2009), 111–122. 1

[DHS00] DUDA R. O., HART P. E., STORK D. G.: *Pattern Classification*. Wiley-Interscience, 2000. 5

[DJ06] DONNER C., JENSEN H. W.: A Spectral BSSRDF for Shading Human Skin. In *Eurographics Workshop/ Symposium on Rendering* (2006), Akenine-Möller T., Heidrich W., (Eds.), Eurographics Association, pp. 409–417. 2, 3, 5

[EH79] EGAN W. G., HILGEMAN T. W.: *Optical Properties of Inhomogeneous Materials*. Academic Press (New York), 1979. 3

[HBF*09] HALL M. A., BOUCKAERT R. R., FRANK E., HOLMES G., PFAHRINGER B., REUTEMANN P., WITTEN I. H.: The WEKA Data Mining Software: An Update. *SIGKDD Explorations 11*, 1 (2009). 6

[HRK10] HUYNH C. P., ROBLES-KELLY A.: Hyperspectral Imaging for Skin Recognition and Biometrics. In *IEEE International Conference on Image Processing* (2010), pp. 2325–2328. 1

[KB04] KRISHNASWAMY A., BARANOSKI G. V. G.: A Biophysically-Based Spectral Model of Light Interaction with Human Skin. *Computer Graphics Forum 23*, 3 (2004), 331–340. 2

[KHA*05] KONG S. G., HEO J., ABIDI B. R., PAIK J. K., ABIDI M. A.: Recent Advances in Visual and Infrared Face Recognition – A Review. *Computer Vision and Image Understanding 97*, 1 (2005), 103–135. 1

[KM31] KUBELKA P., MUNK F.: Ein Beitrag zur Optik der Farbanstriche. *Zeitschrift für technische Physik 12* (1931), 593–601. 2, 3

[MMSP00] MARSZALEC E., MARTINKAUPPI B., SORIANO M., PIETIKINEN M.: A Physics-based Face Database for Color Research. *Journal of Electronic Imaging 9*, 1 (2000), 32–38. 6

[PHPT03] PAN Z., HEALEY G., PRASAD M., TROMBERG B. J.: Face Recognition in Hyperspectral Images. *IEEE Transactions on Pattern Analysis and Machine Intelligence 25*, 12 (2003), 1552–1560. 1, 6, 7

[PMRP08] PELAGOTTI A., MASTIO A. D., ROSA A. D., PIVA A.: Multispectral Imaging of Paintings. *IEEE Signal Processing Magazine 25*, 4 (2008), 27–36. 1

[Raw06] RAWLINGS A. V.: Ethnic Skin Types: Are there Differences in Skin Structure and Function? *International Journal of Cosmetic Science 28*, 2 (2006), 79–93. 1, 3, 6

[RX06] RICHARDS J. A., XIUPING J.: *Remote Sensing Digital Image Analysis: An Introduction*. Springer, Berlin, 2006. 1

[THM99] TSUMURA N., HANEISHI H., MIYAKE Y.: Independent-Component Analysis of Skin Color Image. *Journal of the Optical Society of America A 16*, 9 (1999), 2169–2176. 2

[WA06] WANG H., ANGELOPOULOU E.: Spectral Band Selection for Multispectral Imaging via Average Normalized Information. *Journal of Real-Time Image Processing 1*, 2 (2006), 109–121. 7, 8